Journal of Sound and Vibration (1998) **211**(3), 467–480

ROBUST CONTROL OF ACTIVE CONSTRAINED LAYER DAMPING

A. BAZ

Mechanical Engineering Department, University of Maryland, College Park, MD 20742, U.S.A.

(*Received* 26 *February* 1996, *and in final form* 4 *March* 1997)

Conventional **P**assive **C**onstrained **L**ayer **D**amping (PCLD) treatments with visco-elastic cores are provided with built-in sensing and actuation capabilities to actively control and enhance their vibration damping characteristics. The control gains of the resulting **A**ctive **C**onstrained **L**ayer **D**amping (ACLD) treatments are selected, in this paper, for fully treated beams using the theory of robust controls. In this regard, an optimal controller is designed to accommodate the uncertainties of the ACLD parameters, particularly those of the visco-elastic cores which arise from the variation of the operating temperature and frequency. The controller is also designed to reject the effects of the noise and external disturbances. The theoretical performance of beams treated with the optimally controlled ACLD treatment is determined at different excitation frequencies and operating temperatures. Comparisons are made with the performance of beams treated with PCLD treatments. The results obtained emphasize the potential of the optimally designed ACLD as an effective means for providing broadband attenuation capabilities over a wide range of operating temperatures as compared to PCLD treatments.

1. INTRODUCTION

ACLD treatments have been successfully utilized as effective means for damping out the vibration of various flexible structures (Agnes and Napolitano [1], Azvine *et al*. [2], Baz [3, 4], Baz and Ro [5–9], Edberg and Bicos [10], Plump and Hubbard [11], Shen [12] and Van Nostrand *et al*. [13]. Such effectiveness is attributed to the high energy dissipation characteristics of the ACLD treatments as compared to conventional constrained damping layers (Baz [3, 4] and Chen and Baz [14]). Furthermore, the ACLD treatments combine the simplicity and reliability of passive damping with the low weight and high efficiency of active controls to attain high damping characteristics over broad frequency bands. These characteristics are particularly suitable for suppressing the vibration of critical systems where damping to weight ratio is very important.

The effectiveness of the ACLD treatments is validated experimentally and theoretically using simple proportional and/or derivative feedback of the transverse deflection or the slope of the deflection line of the base structure. The control gains have generally been selected arbitrarily to be small enough to avoid instability problems, computed based on the stability bounds developed by Shen [12] for full ACLD treatments or determined using the optimal control strategies devised by Baz and Ro [9] for partial ACLD treatments. In all these attempts, no effort has been exerted to accommodate the uncertainties in the ACLD parameters, particularly those of the viscoelastic cores which arise from the variation of the operating temperature and frequency. Also, in all these studies the

0022–460X/98/130467 + 14 $25.00/0/sv971315

controllers are designed without any provisions for rejecting the effects that the external disturbances have on the ACLD/beam system.

Therefore, the main objective of the present study is to select the control gains using the theory of robust controls in order to ensure global stability of the ACLD treatment in the presence of parametric uncertainties which may result from variation of the properties of the viscoelastic core of the ACLD due to its operation over wide temperature and frequency ranges. At the same time, the control gains are selected such that the disturbance rejection capabilities of the ACLD treatments are maximized over a desired frequency band.

To achieve such an objective a distributed parameter model is developed using Hamilton's principle to describe the dynamics of beams which are fully treated with ACLD treatments. The model is then used to develop closed form transfer functions of the ACLD treatments which are, in turn, used to select the gains of a robust controller in the frequency domain. The small gain theorem (Dorato *et al*. [15], Dahleh and Diaz-Bobillo [16] and Boyd and Barratt [17]) is utilized, in this regard, to ensure stability in the presence of uncertainty in these transfer functions. The gains are also selected to minimize the $\mathscr{H}_2$-norm of the transfer functions between the external disturbances and the deflections at critical locations along the structure to guarantee optimal disturbance rejection capabilities.

The paper is, therefore, organized in seven sections. In section 1 a brief introduction is given. The concept of active constrained layer damping is presented in section 2. The variational model of ACLD is developed in section 3. In section 4 the transfer functions of ACLD treatment are developed and in section 5 the robust controller is devised. The performance characteristics of ACLD with the optimal robust controller is presented in section 6 and compared with that of conventional PCLD. Section 7 gives a brief summary of the conclusions.

2. THE CONCEPT OF ACTIVE CONSTRAINED LAYER DAMPING

ACLD treatment consists of a conventional *passive* constrained layer damping which is augmented with efficient *active* control means to control the strain of the constrained layer, in response to the structural vibrations as shown in Figure 1. The visco-elastic damping layer is sandwiched between two piezo-electric layers. The three-layer composite ACLD when bonded to the beam acts as a smart constraining layer damping treatment with built-in sensing and actuation capabilities. The sensing, as indicated by the sensor voltage V_s, is provided by the piezo-electric layer which is directly bonded to the beam surface. The actuation is generated by the other piezo-electric layer which acts as an active constraining layer that is initiated by the control voltage V_c. With appropriate strain control, through proper manipulation of V_s, structural vibration can be damped out.

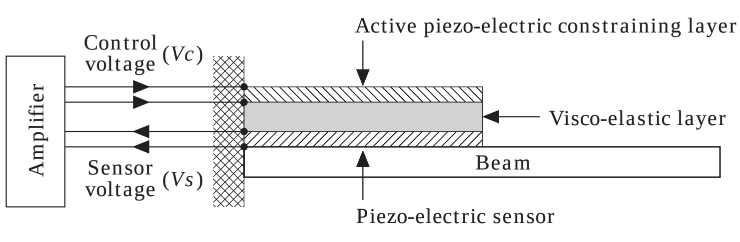

Figure 1. Schematic drawing of the active constrained layer damping.

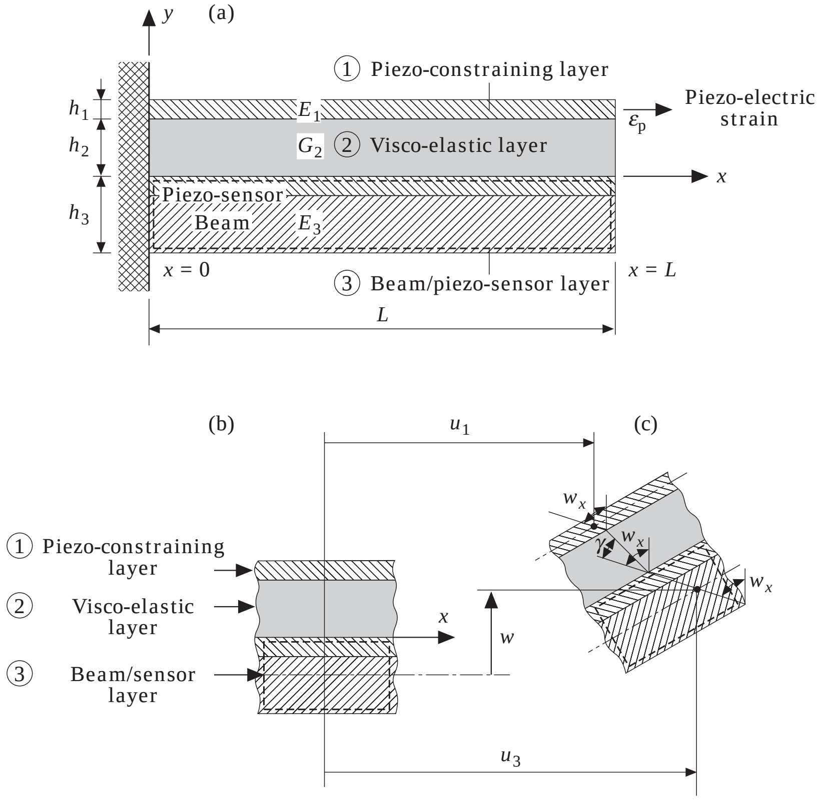

Figure 2. (a) Main parameters of a beam treated with the ACLD; (b) undeflected, (c) deflected.

3. VARIATIONAL MODELLING OF ACTIVE CONSTRAINED LAYER DAMPING

3.1. MODEL BASIC ASSUMPTIONS AND GEOMETRY

Figure 2 shows a schematic drawing of the ACLD treatment of a sandwich beam. It is assumed that the shear strains in both the piezo-electric sensor/actuator layers and in the base beam, together with the longitudinal stresses in the visco-elastic core, are negligible. The transverse displacements w of all points on any cross-section of the sandwiched beam are considered to be equal. Furthermore, the piezo-electric sensor/actuator layers and the base beam are assumed to be elastic and dissipate no energy whereas the core is assumed to be linearly visco-elastic. Also, it is assumed that the thickness and modulus of elasticity of the sensor are negligible compared to those of the base beam.

From the geometry of Figure 2, the shear strain γ in the core is given by

$$\gamma = [hw_x + (u_1 - u_3)]/h_2, \qquad h = h_2 + h_1/2 + h_3/2, \tag{1}$$

where u_1 and u_3 are the longitudinal deflections of the piezo-actuator layer and beam/sensor layer respectively. Also, w denotes the transverse deflection of the beam system. Subscript x denotes partial differentiation with respect to x and h_1, h_2 and h_3 define the thicknesses of the piezo-actuator, the visco-elastic layer, the piezosensor/base beam system respectively.

3.2. THE MODEL

The equations and boundary conditions governing the operation of the beam/ACLD system are obtained by applying Hamilton's principle (Meirovitch [18]):

$$\int_{t_1}^{t_2} \delta\left(\mathrm{KE} - \sum_{i=1}^{3} U_i\right) \mathrm{d}t + \int_{t_1}^{t_2} \delta\left(\sum_{j=1}^{2} W_j\right) \mathrm{d}t = 0, \tag{2}$$

where $\delta(\cdot)$ denotes the first variation in the quantity inside the parentheses. Also, KE, U_i's and W_j's are defined as

$$\mathrm{KE}(\text{kinetic energy}) = 1/2m \int_0^L w_t^2 \,\mathrm{d}x, \tag{3}$$

$$U_1\,(\text{extension energy}) = 1/2K_1 \int_0^L u_{1_x}^2 \,\mathrm{d}x + 1/2K_3 \int_0^L u_{3_x}^2 \,\mathrm{d}x, \tag{4}$$

$$U_2\,(\text{bending energy}) = 1/2D_t \int_0^L w_{xx}^2 \,\mathrm{d}x, \qquad U_3\,(\text{shear energy}) = 1/2G_2' h_2 \int_0^L \gamma^2 \,\mathrm{d}x, \tag{5, 6}$$

$$W_1\,(\text{work done by piezoforces}) = K_1 \int_0^L \varepsilon_p u_{1_x} \,\mathrm{d}x, \tag{7}$$

$$W_2\,(\text{work dissipated in the visco-elastic core}) = -h_2 \int_0^L \tau_d \gamma \,\mathrm{d}x, \tag{8}$$

where m is the mass/unit width and unit length of the sandwiched beam, L is the beam length, $K_1 = E_1 h_1$ and $K_3 = E_3 h_3$ with E_1 and E_3 denoting Young's modulus of the piezo-actuator layer and beam/sensor system. Also, $D_t = (E_1 I_1 + E_3 I_3)$/unit width, with $E_1 I_1$ and $E_3 I_3$ denoting the flexural rigidity of piezo-actuator and the beam/sensor layer, respectively. The storage shear modulus of the visco-elastic layer is G_2' and ε_p is the strain induced in the piezo-electric constraining layer. In this study, ε_p is assumed constant over the entire constraining layer. In equation (8), τ_d is the dissipative shear stress developed by the viscoelastic core. It is given by

$$\tau_d = (G_2' \eta/\omega)\gamma_t = \mathrm{i}(G_2' \eta)\gamma, \tag{9}$$

where η, ω and i denote the loss factor of the visco-elastic core, the frequency and $\sqrt{-1}$, respectively.

The resulting equations of the beam/ACLD system, in dimensionless form, are

$$\bar{u}_{1xx} = a(\bar{u}_1 - \bar{u}_3 + \bar{h}\bar{w}_x), \qquad \bar{u}_{3xx} = ar(-\bar{u}_1 + \bar{u}_3 - \bar{h}r\bar{w}_x), \tag{10, 11}$$

$$\bar{w}_{xxxx} = \bar{\omega}^2\bar{w} + b(\bar{u}_{1x} - \bar{u}_{3x} + \bar{h}\bar{w}_{xx}) = 0, \tag{12}$$

where $a = G_2 L^2/(K_1 h_2)$, $b = G_2 hL^3/(h_2 D_t)$, $\bar{\omega}^2 = m\omega^2 L^4/D_t$, $\bar{h} = h/L$, $\bar{u}_1 = u_1/L$, $\bar{u}_3 = u_3/L$, $\bar{w} = w/L$, $x = x/L$, $r = K_1/K_3$ and $G_2 = G_2'(1 + \mathrm{i}\eta)$.

For a cantilevered beam, Hamilton's principle indicates that the above equations are subject to the following boundary conditions:

$$\text{at } x = 0: \qquad \bar{u}_1(0) = 0, \qquad \bar{u}_3(0) = 0, \qquad \bar{w}(0) = 0, \qquad \bar{w}_x(0) = 0, \tag{13}$$

$$\text{at } x = 1: \quad \bar{u}_{1x}(1) = \varepsilon_p, \quad \bar{u}_{3x}(1) = 0, \quad \bar{w}_{xx}(1) = 0,$$

$$\bar{w}_{xxx}(1) - b[(\bar{u}_1(1) - \bar{u}_3(1) + h\bar{w}_x(1)] = P, \tag{14}$$

where $P = pL^2/D_t$ with p denoting a transverse end load.

It is important here to note that combining equations (10)–(12) by eliminating $\bar{u}_1$ and $\bar{u}_3$ yields a sixth order partial differential equation in the transverse deflection of the beam/ACLD system. The resulting equation is exactly the same as that developed by Mead and Markus [19] to describe the dynamics of a beam treated with conventional PCLD. However, the boundary condition $\bar{u}_{1x}(1)$ is modified to account for the control action generated by the strain ε_p induced by the active constraining layer at the free end of the beam (i.e., at $x = 1$) (Baz [4]).

However, in the present study equations (10)–(12) are manipulated differently to obtain the spatial state space representation of the ACLD/system which is then used to develop the system transfer functions as shown in section 4.

4. TRANSFER FUNCTIONS OF THE ACLD/BEAM SYSTEM

4.1. OVERVIEW

The transfer function approach has been utilized recently to study the stability of ACLD treatments with certain parameters (Shen [12]). The approach has also been adopted in 1986 by Alberts *et al*. [20] to define the stability limits for rotating beams treated with passive constrained layer damping of fixed parameters. In the present study, the transfer function approach is employed to design the controller of the ACLD treatments, in the frequency domain, in order to ensure stability in the presence of parameter uncertainty and guarantee optimal disturbance rejection capabilities.

4.2. THE TRANSFER FUNCTIONS

Equations (10)–(12) are rewritten in the matrix form

$$\mathbf{Z}_x = \mathbf{AZ}, \tag{15}$$

where $\mathbf{Z} = [u_1, u_3, w, w_x, u_{1x}, u_{3x}, w_{xx}, w_{xxx}]^{\mathrm{T}}$ is the spatial state vector of the ACLD/beam system and $\mathbf{A}$ is

$$\mathbf{A} = \begin{bmatrix} 0 & 0 & 0 & 0 & 1 & 0 & 0 & 0 \\ 0 & 0 & 0 & 0 & 0 & 1 & 0 & 0 \\ 0 & 0 & 0 & 1 & 0 & 0 & 0 & 0 \\ 0 & 0 & 0 & 0 & 0 & 0 & 1 & 0 \\ a & -a & 0 & a\bar{h} & 0 & 0 & 0 & 0 \\ -ar & ar & 0 & -a\bar{h}r & 0 & 0 & 0 & 0 \\ 0 & 0 & 0 & 0 & 0 & 0 & 0 & 1 \\ 0 & 0 & \bar{\omega}^2 & 0 & b & -b & b\bar{h} & 0 \end{bmatrix}. \tag{16}$$

The solution of equation (13) gives the spatial state vector $\mathbf{Z}$ at the beam free end as

$$\mathbf{Z}(1) = \mathrm{e}^{\mathbf{A}}\mathbf{Z}(0). \tag{17}$$

Incorporating the boundary conditions of equations (13) and (14) and rearranging the results yields the following two sets of equations:

$$\begin{bmatrix} u_1(1) \\ u_3(1) \\ w(1) \\ w_x(1) \end{bmatrix} = A_1 \begin{bmatrix} u_{1x}(0) \\ u_{3x}(0) \\ w_{xx}(0) \\ w_{xxx}(0) \end{bmatrix}, \qquad \begin{bmatrix} \varepsilon_p \\ 0 \\ 0 \\ P \end{bmatrix} = A_2 \begin{bmatrix} u_{1x}(0) \\ u_{3x}(0) \\ w_{xx}(0) \\ w_{xxx}(0) \end{bmatrix}, \qquad (18, 19)$$

where A_1 and A_2 are given by

$$A_1 = \begin{bmatrix} f_6 - (c + b\overline{h})f_4 - \bar{\omega}^2 f_2 + c\bar{\omega}^2 f & -af_4 + a\bar{\omega}^2 f & a\overline{h}f_4 & a\overline{h}f_3 \\ -cf_4 + c\bar{\omega}^2 f & f_6 - (a + b\overline{h})f_4 - \bar{\omega}^2 f_2 + a\bar{\omega}^2 f & -c\overline{h}f_4 & -c\overline{h}f_3 \\ bf_3 & -bf_3 & -(a+c)f_3 + f_5 & -(a+c)f_2 + f_4 \\ bf_4 & -bf_4 & -(a+c)f_4 + f_6 & -(a+c)f_3 + f_5 \end{bmatrix}$$

and

$$A_2 = \begin{bmatrix} f_7 - (c + b\overline{h})f_5 - \bar{\omega}^2 f_3 + c\bar{\omega}^2 f_1 & -af_5 + a\bar{\omega}^2 f_1 & a\overline{h}f_5 & a\overline{h}f_4 \\ -cf_5 + c\bar{\omega}^2 f_1 & f_7 - (a + b\overline{h})f_5 - \bar{\omega}^2 f_3 + a\bar{\omega}^2 f_1 & -c\overline{h}f_5 & -c\overline{h}f_4 \\ bf_5 & -bf_5 & -(a+c)f_5 + f_7 & -(a+c)f_4 + f_6 \\ b\bar{\omega}^2 f_2 & -b\bar{\omega}^2 f_2 & -(a+c)\bar{\omega}^2 f_2 + \bar{\omega}^2 f_4 & -(a+c)f_5 + f_7 - b\overline{h}f_5 \end{bmatrix}$$

with f is defined as $f(x = 1)$, where $f(x)$ is given by

$$f(x) = \mathfrak{L}^{-1}[1/\{s^2[s^6 - (a + c + b\overline{h})s^4 - \bar{\omega}^2 s^2 + \bar{\omega}^2(a + c)]\}] = (1/\bar{\omega}^2(a + c))x + \sum_{i=1}^{6} R_i\, e^{\delta_i x} \qquad (20)$$

and

$$f_i = [d^i f(x)/dx^i]_{x=1}, \qquad i = 1, \ldots, 7.$$

In equation (20), R_i and δ_i are the residues and the roots of the partial fraction expansion of the polynomial $[s^6 - (a + c + b\overline{h})s^4 - \bar{\omega}^2 s^2 + \bar{\omega}^2(a + c)]$ with s the spatial Laplace operator and $c = ar$.

Equations (18) and (19) are combined by eliminating the unknown boundary conditions at the fixed end, to give

$$\begin{bmatrix} \bar{u}_1(1) \\ \bar{u}_3(1) \\ \bar{w}(1) \\ \bar{w}_x(1) \end{bmatrix} = \mathbf{A}_1 \mathbf{A}_2^{-1} \begin{bmatrix} \varepsilon_p \\ 0 \\ 0 \\ P \end{bmatrix} = \begin{bmatrix} Gu_1\,\varepsilon_p & Gu_1\,p \\ Gu_3\,\varepsilon_p & Gu_3\,p \\ Gw\varepsilon_p & Gwp \\ Gw_x\,\varepsilon_p & Gw_x\,p \end{bmatrix} \begin{bmatrix} \varepsilon_p \\ P \end{bmatrix}. \qquad (21)$$

Equation (21) gives the output deflections $[\bar{u}_1, \bar{u}_3, \bar{w}, \bar{w}_x]$ at the free end in terms of the input control action (ε_p) and the external disturbance (P). Such input/output relationships are represented by the appropriate transfer functions G_{ij}'s between the output i and the input j. These transfer functions are used, in section 5, to design a controller that can generate the control action ε_p such that it stabilizes the ACLD/beam system in the presence of parametric uncertainty and guarantee optimal rejection of the disturbance P.

5. DEVELOPMENT OF THE ROBUST CONTROLLER

5.1. OVERVIEW

Figure 3 shows a block diagram of a robust controller with transfer function K that stabilizes the ACLD/beam system with transfer function G in the presence of multiplicative parameter uncertainty Δ when the system is subjected to an external disturbance p. In Figure 3, w_r is a desirable reference transverse deflection which ideally is set equal to zero.

5.2. SELECTION OF THE CONTROLLER

5.2.1. *Stability*

The small gain theorem (Dorato *et al*. [15], Dahleh and Diaz-Bobillo [16] and Boyd and Barratt [17] is utilized to select the controller K to ensure stability in the presence of uncertainty Δ due to the effect of the operating temperature and frequency on the properties of the visco-elastic cores. Mathematically, the stability is guaranteed if the following small gain inequality is satisfied:

$$|\Delta| < 1/|GK(I + GK)^{-1}| = 1/|T|, \tag{22}$$

where $\Delta = \sup_\theta [(\bar{G} - G)/G]$; ϑ is the set of all operating temperatures. In equation (22), G and $\bar{G}$ denote the nominal and the actual transfer functions of the ACLD/beam system computed at the nominal design temperature and any other operating temperature ϑ respectively. For illustrative purposes and without any loss of generality, G and $\bar{G}$ are selected in this study to be the nominal and actual transfer functions $Gw\varepsilon_p$ and $\bar{G}w\varepsilon_p$ between the control action ε_p and the transverse deflection $w(1)$. Also, T denotes the complementary sensitivity transfer function.

5.2.2. *Disturbance rejection*

The controller transfer function K is selected also to minimize the $\mathscr{H}_2$ norm of the transfer function Gwp between the external disturbance P and the transverse deflection w

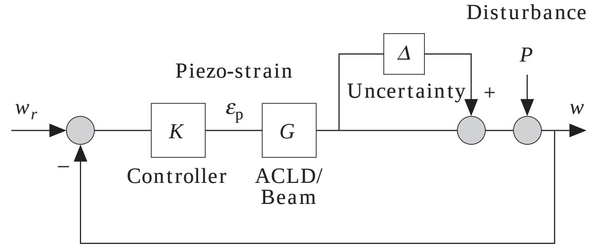

Figure 3. Block diagram of controller, ACLD system with uncertainty and external disturbance.

at the free end of the beam to guarantee optimal disturbance rejection capabilities. Mathematically, this $\mathscr{H}_2$ norm is defined as

$$\| Gwp \|_2^2 = 1/2\pi \int_0^\infty G^*wpGwp \, \mathrm{d}\omega, \tag{23}$$

with G^*wp denoting the complex conjugate transpose of Gwp.

5.2.3. *Controller optimal transfer function*

Mathematically, the problem of finding the controller optimal transfer function K is formulated as

$$\left\langle \begin{array}{c} \text{Find controller transfer function } K \\ \text{to minimize } \| Gwp \|_2^2 \\ \text{such that } |\Delta| < 1/|GK(I + GK)^{-1}| \end{array} \right\rangle \tag{24}$$

The Powell conjugate direction augmented with the penalty function method is used to search for the optimal coefficients of the numerator and denominator of the controller transfer function K (Rao [21], Boyd and Barratt [17]).

6. PERFORMANCE OF THE ACLD WITH THE ROBUST CONTROLLER

6.1. MATERIALS

The effectiveness of the robust control of the ACLD treatment is demonstrated using a cantilevered steel beam which is 1·0 m long, 1·25 cm thick and 10 cm wide. The beam is treated with an acrylic base visco-elastic material which is 1·50 cm thick. The visco-elastic material used is Dow Corning Sylgard 188 whose shear modulus and loss factor are shown in Figures 4(a) and 4(b) respectively at different operating temperatures and frequencies (Nashif *et al*. [22]). The figures demonstrate clearly that the complex modulus of the visco-elastic core varies dramatically, by more than ten fold, when the operating temperature is varied from 75°F by ± 25°F and the frequency is scanned over a 2500 Hz bandwidth. Such pronounced changes in the properties of the viscoelastic layer introduce significant uncertainties in the parameters of the ACLD/beam system.

The viscoelastic core is sandwiched between two ceramic piezo-electric films (PTS-1195, Piezo-electric Products, Meutchen, NJ) whose thickness h_1, Young's modulus E_1 and piezo-electric strain constant are 0·625 cm, 63 GN/m^2 and $18{\cdot}6 \times 10^{-11}$ m/V. This results in the following values for the main parameters: $r = K_1/K_3 = 0{\cdot}15$, $h = 0{\cdot}035$ m, $D_t = 3{\cdot}55\text{E}4$ Nm and $m = 182$ kg/m.

6.2. OPEN-LOOP CHARACTERISTICS OF THE ACLD/BEAM SYSTEM

Figure 5(a) shows the effect of the operating temperature and frequency on the magnitude of the open loop transfer function $Gw\varepsilon_p$ of the ACLD/beam system. It is evident that the nominal transfer function $Gw\varepsilon_p$, set at 75°F, is significantly different from the actual transfer functions $\bar{G}w\varepsilon_p$ at 50°F or 100°F. The normalized differences between the nominal and actual transfer functions define the parameter uncertainties Δ_{50} and Δ_{100} of the system as shown in Figure 5(b) with $\Delta_\vartheta = [(\bar{G}_\vartheta - G)/G]$.

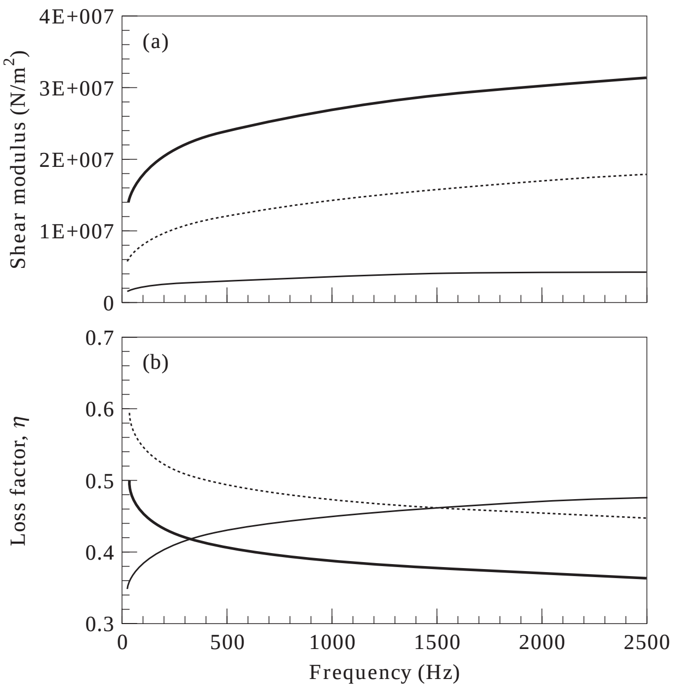

Figure 4. Complex modulus of the viscoelastic core: (a) shear modulus, (b) loss factor; ——, 50°F; – – –, 75°F; —, 100°F.

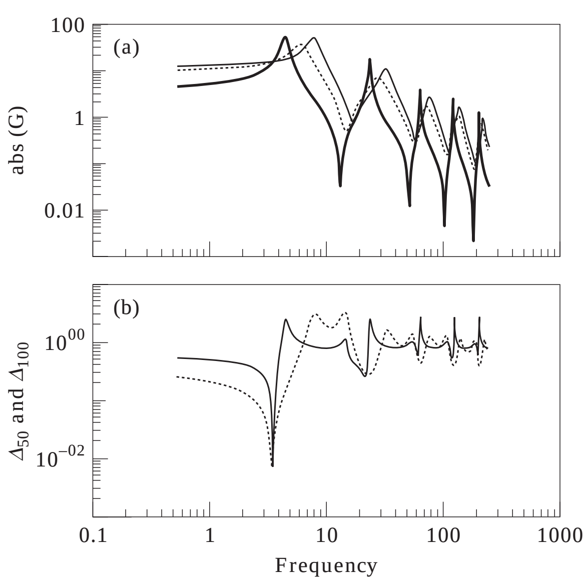

Figure 5. Effect of temperature and frequency on (a) open-loop transfer function (- - - -, $G75$; —, $G50$; ——, $G100$) and (b) parameter uncertainty (- - - -, Δ 50; —, Δ 100).

TABLE 1

Stability limits and $\|Gwp\|_2^2$ for P, I and D controllers

Controller	Uncontrolled	P	I	D
stable gain ⩽	—	0·01	0·05	0·001
$\|Gwp\|_2^2$	0·108	0·108	0·086	0·134

6.3. PERFORMANCE WITH SIMPLE P, I AND D CONTROLLERS

The use of simple P, I or D control actions, each separate or combined, to control the uncertain ACLD/beam system is found to be ineffective as suggested by the results summarized in Table 1.

Table 1 indicates that in order to ensure stability, in the presence of the set uncertainties, the control gains become very small to produce any pronounced control action as in the case of the P and I controllers. In the case of the D controller, the stable performance of the closed loop is found to be even worse than that of the open loop.

6.4. PERFORMANCE OF A PREFERRED CONTROLLER

A simple controller is suggested with the transfer function

$$K = g(s + a_0)/s^2, \tag{25}$$

where the gain g and the parameter a_0 are determined optimally according to the formulation given by equation (24). Such simple controller is selected to maintain the simplicity and hence the practicality of implementation of the ACLD treatments in real systems.

Figure 6 shows the stability boundary and the iso-$\mathscr{H}_2$ norm contours plotted on the $(g - a_0)$-plane. Displayed also in the figure is the optimal combination of g and a_0 at which

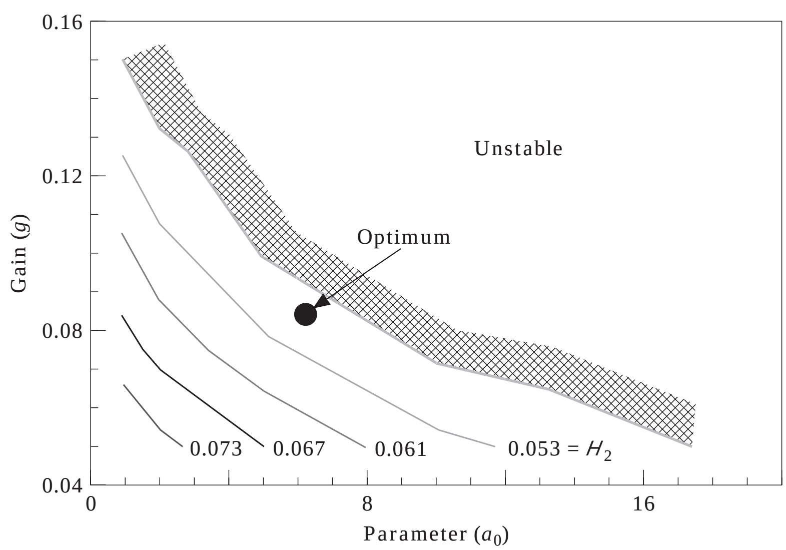

Figure 6. The stability boundary and the iso-$\mathscr{H}_2$ norm contours of the ACLD/beam system in the $(g - a_0)$-plane.

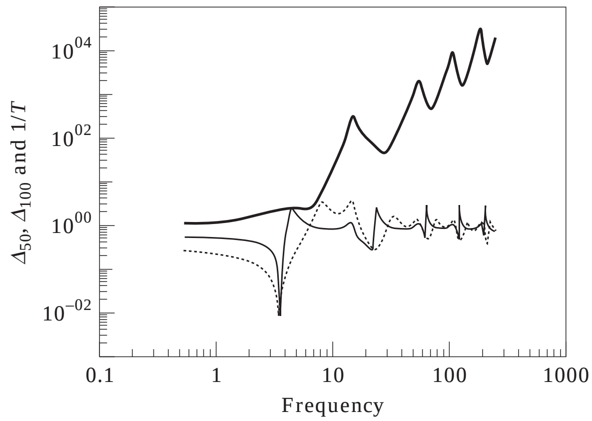

Figure 7. Graphical representation of the small gain inequality (- - - -, Δ 50; —, Δ 100; ▬▬, $1/T$).

the $\mathscr{H}_2$ norm ($\| Gwp \|_2^2$) attains a minimum. At this optimal design point $g = 0{\cdot}0875$, $a_0 = 6$ and $\mathscr{H}_2$ norm is 0·047 which is 44% of that of the uncontrolled system.

It is important here to note that the devised optimal controller design satisfies the small gain theory inequality (22) as indicated in Figure 7. Also, such a design has favorable sensitivity S and co-sensitivity T characteristics as shown in Figure 8. The sensitivity is very low at low frequencies to ensure good disturbance rejection capabilities and the co-sensitivity become slow at higher frequencies to guarantee suppression of measurement noise (Dahlaeh and Diaz-Bobillo [16] and Boyd and Barratt [17]).

Figure 9 shows the performance of the optimal controller at 50°F, 75°F and 100°F. It is evident that the controller has been effective in damping out the vibration of the ACLD/beam system within its bandwidth.

7. CONCLUSIONS

This paper has presented a variational formulation of the dynamics of beams which are fully treated with active constrained layer damping treatments. The equations and the boundary conditions governing the performance of this class of surface treatment are presented using Hamilton's principle. These equations are used to derive expressions for

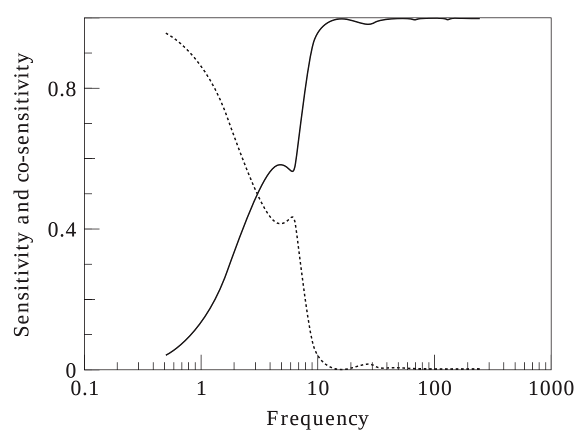

Figure 8. The sensitivity and co-sensitivity of the optimal controller; ——, s; - - - -,, T.

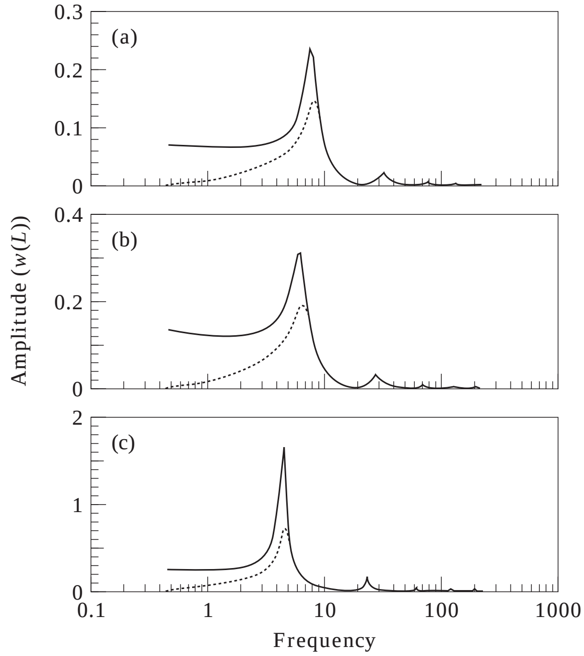

Figure 9. Performance of robust controller at different temperatures: (a) 50°F, (b) 75°F, and (c) 100°F. —, Uncontrolled; - - - -, controlled.

distributed parameter transfer functions of the ACLD/beam system and devise a robust control strategy which is stable in the presence of parameter uncertainty. In this manner and as no mode truncations are involved, the stability of the controller is guaranteed for all the modes of vibration. Furthermore, the developed control strategy ensures also optimal disturbance rejection capabilities. A numerical example is presented to demonstrate the effectiveness of the robust controller in damping out structural vibrations when the ACLD/beam system operates over wide temperature and frequency ranges. Under similar operating circumstances, it is found that simple P, I and D controllers fail in producing any significant vibration control when the stability constraints are imposed over the entire range of operation.

It is important here to note that although in the present study a low order controller is used to illustrate the utility of the robust control concepts in the control of ACLD/beam systems, a higher order controller can equally be devised to damp out the vibration over wider frequency ranges. The low order controller is selected, however, to maintain the simplicity and hence the practicality of implementation of the ACLD treatments in real systems.

Also, to extend the applicability of the developed robust controller to account for general disturbance spectra, appropriate frequency dependent weighting transfer functions W_s can be used to put bounds on the sensitivity S as outlined by Lewis [23], Boyd and Barratt [17] and Shahian and Hassul [24]. Similar weighting transfer functions W_T can be set to impose constraints on the co-sensitivity T to account for the frequency spectra of the sensor dynamics and the measurement noise. In this manner, the weighting transfer functions W_s and W_T are used to shape the sensitivity S and co-sensitivity T characteristics in the frequency domain. These frequency dependent constraints should be added to the optimal controller problem, given by equation (24), before the search is carried out for the controller optimal transfer function K.

ACKNOWLEDGMENTS

This work is funded by the U.S. Army Research Office (Grant number DAAH-04-93-G-0202). Special thanks are due to Dr. Gary Anderson, the technical monitor, for his invaluable technical inputs.

REFERENCES

1. G. S. Agnes and K. Napolitano 1993 *Proceedings of the* 34*th SDM Conference*, pp. 3499–3506. Active constrained layer viscoelastic damping.
2. B. Azvine, G. Tomlinson and R. Wynne 1994 *Proceedings of Smart Structures and Materials Conference on Passive Damping* (editor C. Johnson) **2193**, 138–149, Orlando, Florida. Initial studies into the use of active constrained layer damping for controlling resonant vibration.
3. A. Baz 1996 *U.S. Patent* 5485053. Active constrained layer damping.
4. A. Baz 1996 *Journal of Smart Materials and Structures*. Optimization of energy dissipation characteristics of active constrained layer damping.
5. A. Baz and J. Ro 1993 *Conference of Engineering Sciences Society*, *ASME-AMD*, Charlottesville, VA **167**, 61–80. Partial treatment of flexible beams with active constrained layer damping.
6. A. Baz and J. Ro 1993 *Ninth VPI & SU Conference on Dynamics and Control of Large Structures*, Blacksburg, VA, 345–358. Finite element modeling and performance of active constrained layer damping.
7. A. Baz and J. Ro 1994 *Sound and Vibration Magazine* **28**, 18–21. Actively-controlled constrained layer damping.
8. A. Baz and J. Ro 1995 *Shock and Vibration Journal* **2**(1), 33–42. Performance characteristics of active constrained layer damping.
9. A. Baz and J. Ro 1995 *ASME Journal of Vibration and Acoustics* **117** B, 135–144. Optimum design and control of active constrained layer damping.
10. D. Edberg and A. Bicos 1992 *Conference on Active Materials and Adaptive Structures* (editor G. Knowles) IOP Publishing Ltd., Bristol, England, 377–382. Design and development of passive and active damping concepts for adaptive structures.
11. J. Plump and J. E. Hubbard 1986 *12th International Congress on Acoustics* **D41**, Toronto, Canada. Modeling of an active constrained layer damper.
12. I. Y. Shen 1994 *ASME Journal of Vibration and Acoustics* **116**, 341–349. Hybrid damping through intelligent constrained layer treatments.
13. W. Van Nostrand, G. Knowles and D. Inman 1994 *Proceedings of Smart Structures and Materials Conference on Passive Damping* (editor C. Johnson) **2193**, 126–137, Orlando, Florida. Finite element modeling for active constrained-layer damping.
14. T. Chen and A. Baz 1996 *Conference on Smart Materials and Structures* **2715**, 256–268, *San Diego*, *CA*, Performance characteristics of active control with passive constrained layer damping versus active constrained layer damping.
15. P. Dorato, C. Abdallah and V. Cerone 1995 *Linear Quadratic Control*: *An Introduction*. Englewood Cliffs, NJ: Prentice Hall.
16. M. Dahlaeh and I. Diaz-Bobillo 1995 *Control of Uncertain Systems*: *A Linear Programming Approach*. Englewood Cliffs, NJ: Prentice Hall.
17. S. Boyd and C. Barratt 1991 *Linear Controller Design*: *Limits of Performance*. Englewood Cliffs, NJ: Prentice Hall.
18. L. Meirovitch 1967 *Analytical Methods in Vibrations*. New York: MacMillan.
19. D. J. Mead and S. Markus 1969 *Journal of Sound and Vibration* **10**, 163–175. The forced vibration of a three-layer, damped sandwich beam with arbitrary boundary conditions.
20. T. Alberts, S. Dickerson and W. Book 1986 *In Robotics*: *Theory and Applications*. New York: ASME; pp. 23–30. On the transfer function modeling of flexible structures with distributed damping.
21. S. Rao 1984 *Optimization Theory and Applications*. New Delhi, India: J. Wiley. Second edition.

22. N. Nashif, D. I. Jones and J. P. Henderson 1985 *Vibration Damping*. New York: J. Wiley.
23. F. Lewis 1992 *Applied Optimal Control and Estimation*: *Digital Design and Implementation*. Englewood Cliffs, NJ: Prentice Hall.
24. B. Shahian and M. Hassul 1993 *Control System Design Using MATLAB*. Englewood Cliffs, NJ: Prentice Hall.

NOMENCLATURE

a	$G_2 L^2/(K_1 h_2)$
A	system matrix (equation (16))
b	$G_2 hL^3/(h_2 D_t)$
c	ar
D_t	combined flexural rigidity of sandwiched beam/unit width
$E_{1,3}$	moduli of elasticity of piezo-actuator and beam
f	spatial function (equation (20))
f_i	ith derivative of f
g	control gain
G	transfer function of ACLD/beam system
G_{ij}	transfer function of ACLD/beam system between input j and output i
G_2	complex shear modulus of the visco-elastic core
$h_{1,2,3}$	thicknesses of piezo-actuator, visco-elastic core and beam
i	$\sqrt{-1}$
$k_{1,3}$	$E_1 h_1$ and $E_3 h_3$
K	transfer function of controller
KE	kinetic energy
L	beam length
m	mass of sandwiched beam/unit length and unit width
p	transverse load applied to free end of beam
P	pL^2/D_t
r	K_1/K_3
R_i	residues of partial fraction expansion
s	spatial Laplace operator
S	sensitivity function ($=1-T$)
t	time
T	co-sensitivity function
$u_{1,3}$	longitudinal deflection of neutral axes of piezo-actuator and beam layer
U_i	potential energy
w	transverse deflection of sandwiched beam
w_r	reference transverse deflection
W_i	work done
$W_{s,T}$	weighting matrices to shape S and T characteristics
x	position along beam
Z	spatial state-space vector

Greek symbols

γ	shear strain of visco-elastic core
$\delta(\cdot)$	first variation
δ_i	roots of characteristic equation of ACLD/beam system
Δ	parameter uncertainty (equation (21))
ε_p	strains of piezo-actuator
η	loss factor
ϑ	temperature
τ_d	dissipative shear stress
ω	frequency